

Abstract-

Report Documentation Page

Report Date 25OCT2001	Report Type N/A	Dates Covered (from... to) -
Title and Subtitle Image Segmentation in MRI Using True T1 and True PD Values		Contract Number
		Grant Number
		Program Element Number
Author(s)		Project Number
		Task Number
		Work Unit Number
Performing Organization Name(s) and Address(es) Institute of Biomedical Engineering, Bogazici University, Istanbul, Turkey		Performing Organization Report Number
Sponsoring/Monitoring Agency Name(s) and Address(es) US Army Research, Development & Standardization Group (UK) PSC 802 Box 15 FPO AE 09499-1500		Sponsor/Monitor's Acronym(s)
		Sponsor/Monitor's Report Number(s)
Distribution/Availability Statement Approved for public release, distribution unlimited		
Supplementary Notes Papers from the 23rd Annual International Conference of the IEEE Engineering in Medicine and Biology Society, October 25-28, 2001, held in Istanbul, Turkey. See also ADM001351 for entire conference on cd-rom., The original document contains color images.		
Abstract		
Subject Terms		
Report Classification unclassified	Classification of this page unclassified	
Classification of Abstract unclassified	Limitation of Abstract UU	
Number of Pages 4		

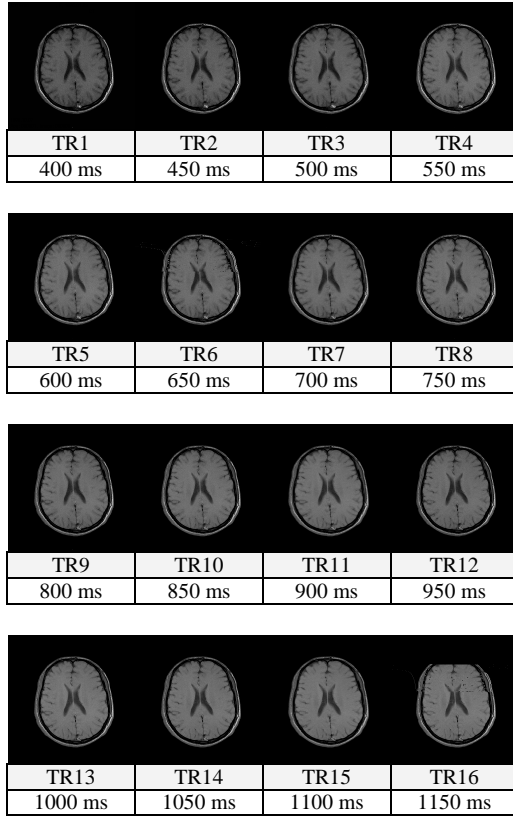


Fig. 1. Spin echo images produced at successive TR times with short TE.

The images were taken from slices of 4 mm thickness and their sizes are 256 x 256.

The pixel values in 16 images were plotted against TR values as shown in Fig. 2.

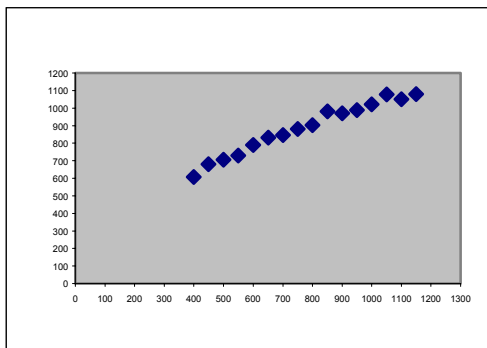


Fig. 2. Pixel value versus TR.

At the next step, Levenberg-Marquardt Method is applied to the data and T_1 and PD values were estimated.

A sample data together with the fitted exponential curve and the estimated parameters, P1 and P2 (they stand for PD and T_1) is shown in Fig. 3.

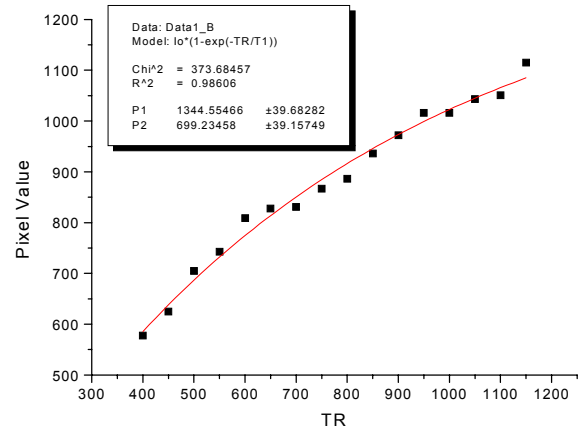


Fig. 3. A sample dataset of estimated parameters and the best fit.

The fitting algorithm was applied to all pixels and (T_1 , PD) values were recorded for each coordinate. By using these estimated values the calculated T_1 and calculated PD image (see Fig. 4) are created.

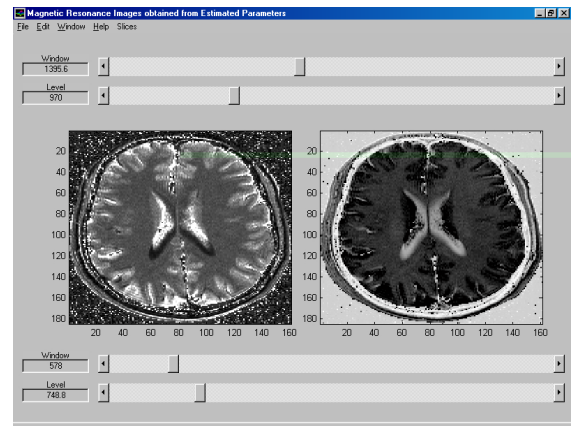


Fig. 4. Calculated T_1 and calculated PD images.

The image on the left is the true T_1 image, next to it is the true PD image.

B. Segmentation of Weighted and Calculated Images

In my research I used maximum likelihood method to choose the class that each pixel of our image belongs. First, two scatter diagrams are produced where each data point is a function of T_1 and PD. One of these scatter diagrams is achieved by using the T_1 -weighted (TR1=400 ms.) and PD-weighted (TR16=1150 ms.) images (Fig. 5).

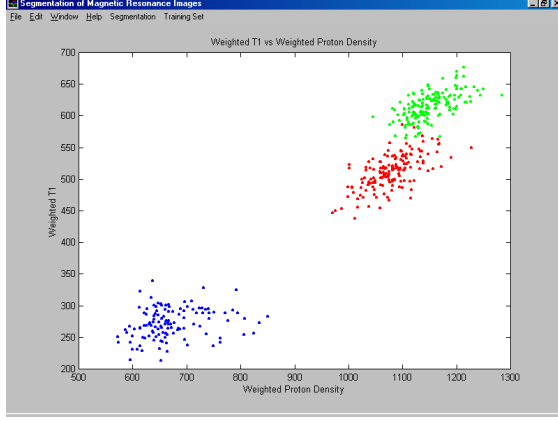


Fig. 5. Scatter diagram of pixels chosen from T₁-weighted and PD-weighted images.

Blue dataset is CSF, red dataset is GM, and green dataset is WM. The training dataset that will be used in weighted image segmentation is created by choosing some coordinates on the brain slices. The same coordinates are also necessary to set up the training dataset that will be used in calculated image segmentation. That training dataset is shown in Fig. 6.

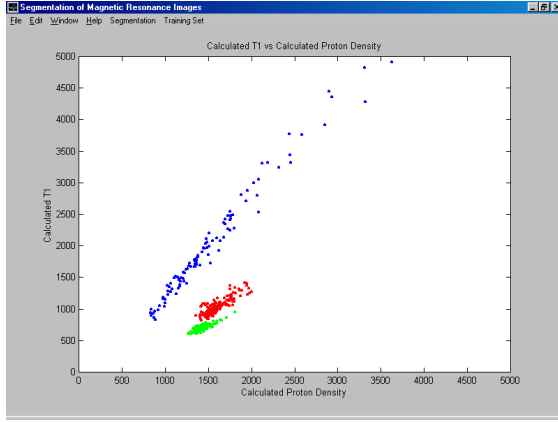


Fig. 6. Scatter diagram of pixels chosen from true T₁ and true PD images.

Next the multivariate Gaussian density functions (Fig. 7 and Fig. 8) of both the weighted and the calculated datasets are found by using (1).

$$f_{X_1, X_2}(x_1, x_2) = \frac{1}{\sqrt{(2\pi)^n \det(C_{xx})}} e^{-\frac{1}{2}(x-\mu)^T C_{xx}^{-1} (x-\mu)} \quad (1)$$

where \mathbf{x} and μ_x are each 2 by 1 vectors with components x_k and $E\{X_k\}$, respectively, for $1 \leq k \leq 2$ and C_{xx} is the associated 2 by 2 covariance matrix. The symbol $\det(C_{xx})$ denotes the determinant of the covariance matrix.

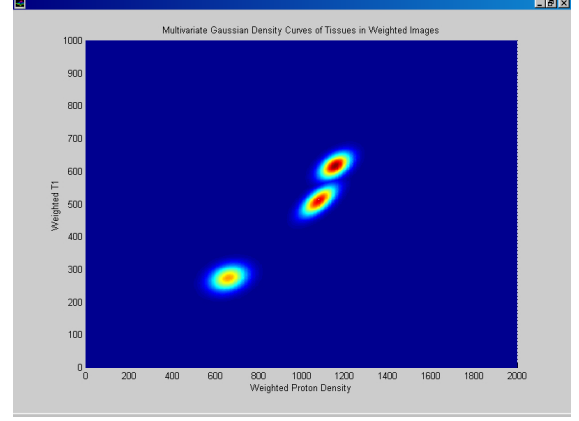


Fig. 7. The multivariate Gaussian density function of the weighted dataset.

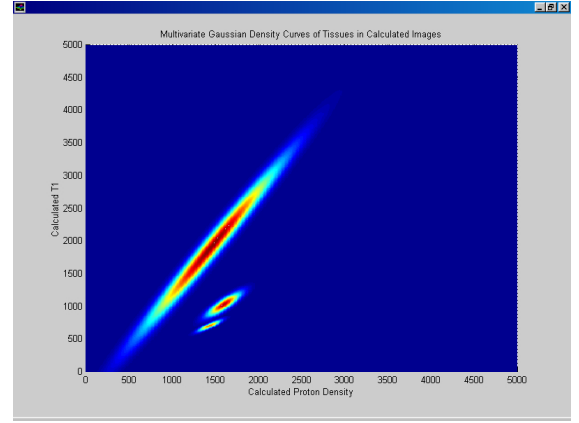


Fig. 8. The multivariate Gaussian density function of the calculated dataset.

The segmentation algorithm based on the maximum likelihood classification method that utilizes the multivariate Gaussian density functions is applied to the 4 human head slices, one of which is illustrated in Fig. 9 and Fig. 10.

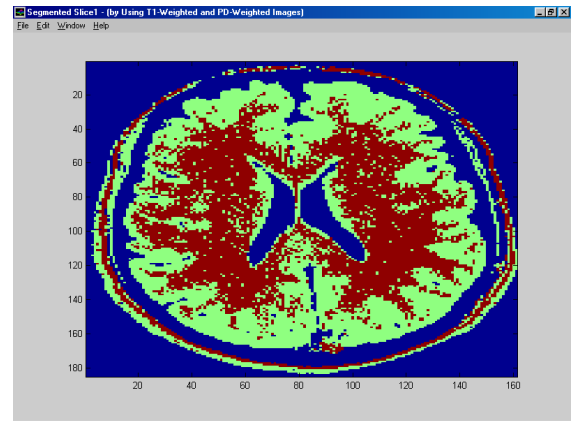


Fig. 9. Segmented slice by using weighted dataset.

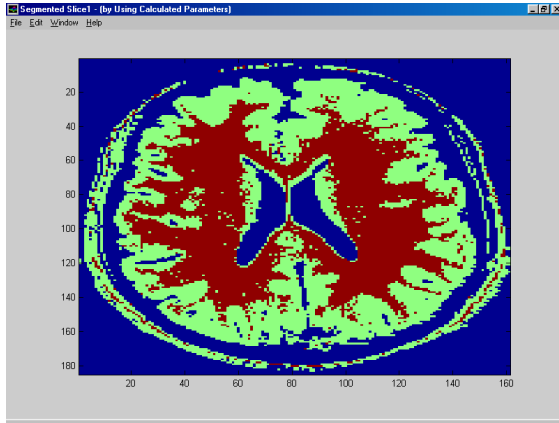


Fig. 10. Segmented slice by using calculated dataset.

III. RESULTS

To evaluate the reliability of the segmentation algorithm, 400 test pixels are chosen from each tissue (CSF, WM, and GM). The newly chosen pixels (test pixels) are different from the ones that constituted the training dataset. They are used as input to the segmentation algorithm and the results of segmentation are arranged in confusion matrices as shown in Table 1 and Table 2. The tissues from which the test pixels are chosen are placed at the first column of these tables. The first row shows the distribution of segmentation among three tissues. For example, in the second row, 348 test pixels are classified as CSF, 52 test pixels are classified as GM, and 0 test pixel is classified as WM from 400 test pixels chosen from CSF.

		Result of segmentation		
	Tissue	CSF	GM	WM
Tissues from which the pixels are chosen	CSF	348	52	0
	GM	0	356	44
	WM	0	40	360

		Result of segmentation		
	Tissue	CSF	GM	WM
Tissues from which the pixels are chosen	CSF	360	40	0
	GM	0	388	12
	WM	0	8	392

IV. CONCLUSION

To evaluate the correctness of the segmentation algorithm the confusion matrix method is used. The test pixels are chosen from the coordinates that are not used when setting up the training datasets. To be certain at doing this, the training datasets are constituted from the tissues on the left lobe of the brain, and the test pixels are chosen from the tissues on the right lobe of the brain. The segmentation done with the calculated datasets gave more satisfactory results than the segmentation done with the weighted datasets.

In this study, development of a segmentation algorithm by using calculated T_1 and calculated PD images is aimed. For this purpose the true T_1 and true PD images are produced by finding the best exponential curves fitting to the images taken from an MR imager, and the segmentation is achieved by using the maximum likelihood method. We conclude that the segmentation done with the calculated datasets gave very satisfactory results and that it will be helpful in detecting the tumors in the brain.

REFERENCES

- [1] Paty, D. W., D. K. B. Li, "Interferon beta-1b is effective in relapsing-remitting multiple sclerosis. ii. MRI analysis results of a multicenter, randomized, double-blind, placebo-controlled trial", *Neurol.*, vol. 43, pp. 662-667, April 1993.
- [2] Paty, D. W., "Interferon beta-1b in the treatment of multiple sclerosis: Final outcome of the randomized controlled trial", *Neurol.*, vol. 45, pp. 1277-1285, July 1995.
- [3] Johnston, B., M. S. Atkins, "Segmentation of multiple sclerosis lesions in intensity corrected multispectral MRI", *IEEE Trans. Med. Imag.*, vol. 15, pp. 154-169, April 1996.
- [4] Zi" -1.14I en94.1(osT)67(9, A)45.4(.10.1 (P)7[(.,Br)-4.6(.10.1 M.Da
IEEE Trans. Med. Imag. (2006) 25(10):1277-1285
doi:10.1109/TMI.2006.2811641
Received August 27, 2006; revised May 1, 2007; accepted May 1, 2007.
This work was supported by the National Natural Science Foundation of China (Grant No. 81073001).
Corresponding author: Dr. Li, E-mail: lili@pku.edu.cn
Digital Object Identifier 10.1109/TMI.2007.911641